ARTICLE IN PRESS

Deep-Sea Research II ∎ (∎∎∎∎) ∎∎∎–∎∎∎

Contents lists available at ScienceDirect

Deep-Sea Research II

journal homepage: www.elsevier.com/locate/dsr2

Investigation of Arctic sea ice and ocean primary production for the period 1992–2007 using a 3-D global ice–ocean ecosystem model

Meibing Jin [a,]*, Clara Deal [a], Sang H. Lee [b], Scott Elliott [c], Elizabeth Hunke [c], Mathew Maltrud [c], Nicole Jeffery [c]

[a] International Arctic Research Center, University of Alaska Fairbanks, 930 Koyukuk Drive, Fairbanks, AK 99775, USA
[b] Department of Oceanography, Pusan National University, Pusan 609-735, South Korea
[c] Los Alamos National Lab, New Mexico, USA

ARTICLE INFO

Keywords:
Primary production
Arctic
Ice–ocean model
Ecosystem model
Climate change

ABSTRACT

In the Arctic Ocean, both phytoplankton and sea ice algae are important contributors to primary production and the arctic food web. An ice algal ecosystem model was added to fully couple with the global physical model POP-CICE (Parallel Ocean Program-Los Alamos Sea Ice Model) and the open-ocean pelagic ecosystem model. The physical model captured the seasonal and interannual variations of northern hemispheric sea ice extent and area measured by satellite remote sensing for the model period of 1992–2007. The model results showed a reasonable mean seasonal cycle of ice algal production from March to May and subsequent ocean production from May to September in the Arctic. The ice algal production, although smaller than that of the ocean, is of ecological importance as a food source for higher trophic levels during the long arctic winter before ice melt. The simulated mean open-ocean upper 100 m primary production within the Arctic Circle was 413 ± 88 T g C yr^{-1} in the years 1998–2006, close to the remote sensing derived estimate of 419 ± 33 T g C yr^{-1} but with higher interannual variations. The mean sea ice algal production in the Northern Hemisphere from 1998 to 2007 was 21.3 T g C yr^{-1}, which is in the range of multi-observational estimations of 9–73 T g C yr^{-1} based on in situ measurements. Model-data comparisons were conducted with various regional observations and the observed trend of temporal and spatial variation of the primary production. The model results compared well with the following observations and observed trends: (1) an increase of ocean primary production from 2003 to 2007 in the arctic open water areas as derived from remote sensing data; (2) regional annual ice and ocean primary production measured in the Bering and Chukchi seas and Canadian Basin; (3) primary production rate with phytoplankton size composition and Chl-a concentration along an arctic cruise track in the Chukchi Sea and Canadian Basin from August 2 to September 7, 2008; and (4) observed decadal changes of ocean primary production from the 1990s to 2007 due to rising temperature and increasing open-ocean area in the western Arctic. The changes are shown as a trend of a northward shift of production, with a decrease in the Bering Sea and an increase in the Arctic shelf.

1. Introduction

The Arctic Ocean as an iconic indicator and amplifier of global warming has experienced rapid reduction of sea ice in the last several decades, and it is predicted that a complete loss of summer sea ice will occur sometime between 2050 and 2100 (Walsh, 2008). However, we do not yet fully understand the impacts that reduced sea ice cover will have on pan-Arctic marine primary production (Pabi et al., 2008). The open ocean primary production estimated using a model based on recent remote sensing data in the Arctic Ocean in 2003–2007 changed significantly due to an increase of open water area, temperature, and growing season (Arrigo et al., 2008b). These changes have not included the ice algal primary production, which contributes 4–26% to total primary production in seasonally ice-covered arctic seas (Legendre et al., 1992) and >50% in perennially ice-covered waters (Gosselin et al., 1997). Not only is the total ocean production changing under a warming climate in the Arctic, but also the size composition of phytoplankton is shifting toward smaller algae, according to recent observations (Li et al., 2009).

The sea ice algal ecosystem is tightly coupled with the pelagic ecosystem in the Arctic, and the ice-based food web extends from

* Corresponding author.
E-mail address: mjin@alaska.edu (M. Jin).

0967-0645/$ - see front matter © 2011 Elsevier Ltd. All rights reserved.
doi:10.1016/j.dsr2.2011.06.003

Please cite this article as: Jin, M., et al., Investigation of Arctic sea ice and ocean primary production for the period 1992–2007 using a 3-D global ice–ocean ecosystem model. Deep-Sea Research II (2011), doi:10.1016/j.dsr2.2011.06.003

primary producers to marine mammals (Bluhm and Gradinger, 2008). A vertical 1-D ice–ocean coupled ecosystem model (Jin et al., 2009) revealed that the ecosystem in the marginal ice zone in the Bering Sea responded to climate changes in terms of the timing, magnitude, and species composition of the primary production after climate regime shift in 1977. The roles of ice algae in the arctic food web are not replaceable by pelagic production due to the different timing of the blooms. The two types of production are linked, as they are both regulated by available nutrients in the ocean. Sea ice algae usually grow at the sea ice bottom skeletal layer in the spring (Jin et al., 2006a) before ice melting and may trigger ice-associated phytoplankton blooms in the open water (Jin et al., 2007). Modeling studies of the arctic basin-wide ecosystem have been rare and lack the sea ice algae component (e.g., Walsh et al., 2005; Zhang et al., 2010). The few ecosystem model applications including sea ice habitats are still in the vertical 1-D setting (e.g., Arrigo et al., 1993, 1997; Arrigo and Sullivan, 1994; Vezina et al., 1997; Lavoie et al., 2005; Jin et al., 2006a).

The goal of this work is to develop a 3-D ecosystem model with both sea ice algal and pelagic habitats to investigate how the coupled ice–ocean ecosystem varies in response to climate changes in the Arctic. The model is developed on the basis of the global ocean pelagic ecosystem model (Moore et al., 2004) embedded in the CCSM climate model. A sea ice algal ecosystem model component based on Jin et al. (2006a, 2007, 2009) was written into the Los Alamos National Laboratory (LANL) sea ice model (CICE) (Hunke and Lipscomb, 2008; Hunke and Bitz, 2009) and first tested with CICE-standalone with a mixed-layer ocean model and climatologic ocean surface nutrients (Deal et al., in press). In this study, the CICE and ice algal ecosystem models are fully coupled with the Parallel Ocean Program (POP) and the pelagic ocean ecosystem model evolved from Moore et al. (2004).

The POP and CICE have been widely used in different ice and ocean simulation applications and extensively documented in various literatures (see publications at http://climate.lanl.gov/Models/). Therefore, their equations and numerical solutions are not repeated here. The following sections focus on (1) the coupled ice–ocean-ecosystem model (implementation of the ice algal ecosystem in CICE and its coupling with a pelagic ecosystem), (2) numerical forcing, initial conditions for the coupled physical–biological model, (3) model results in comparison with observations, and discussion, and (4) conclusions.

2. The coupled sea ice–ocean ecosystem model

The ice algal model of Jin et al. (2006a) includes four equations for the four components: ice algae, NO_3, NH_4 in unit of mmol N/m^3,

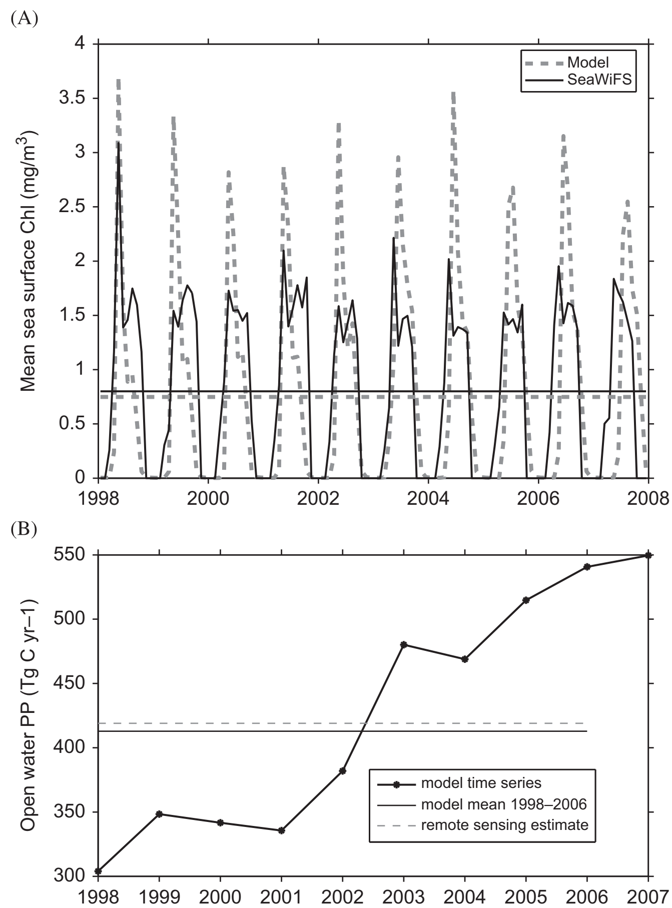

Fig. 2. (A) Comparison of modeled and SeaWiFS monthly mean sea surface Chl-a in the open water within the Arctic Circle (north of 66.56°N). The two horizontal lines are the long-term (1998–2007) mean of the modeled and SeaWiFS Chl-a. (B) Time series of modeled annual upper ocean 100 m integrated primary production in the open water within the Arctic Circle. The mean open water upper 100 m primary production of 1998–2006 was estimates by Pabi et al. (2008) using remote sensing Chl-a and an algorithm developed for the Arctic.

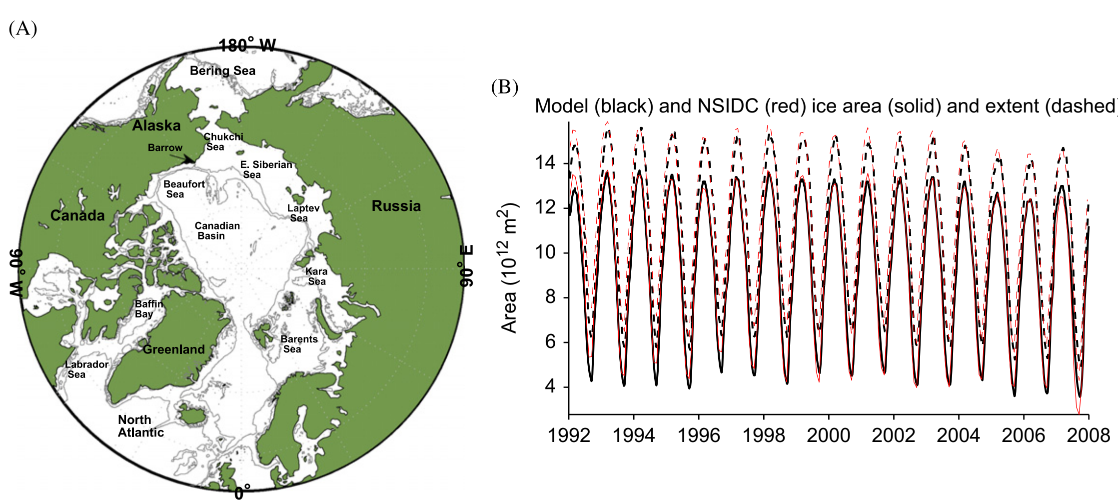

Fig. 1. (A) Pan-Arctic map with the geographic names mentioned in this paper (contour lines are 150 and 1000 m). (B) Comparison of modeled and NSIDC sea ice area and extent.

Please cite this article as: Jin, M., et al., Investigation of Arctic sea ice and ocean primary production for the period 1992–2007 using a 3-D global ice–ocean ecosystem model. Deep-Sea Research II (2011), doi:10.1016/j.dsr2.2011.06.003

and Si in unit of mmol Si/m^3. These equations are applied to the bottom 3 cm of each ice thickness category in the CICE. (Two other components, DMS and DMSP, are also calculated based on the primary production of ice algae, but they are not discussed in the study.) Currently, CICE partitions the ice pack in each grid cell into a five-category ice thickness distribution, with four ice layers and one snow layer in each category. The thickness category ranges are 0–0.64, 0.64–1.39, 1.39–2.47, and 2.47–4.57 m, and greater than 4.57 m (Hunke and Bitz, 2009).

The horizontal advection of the ecosystem variables are handled like other tracers in the CICE. There is a flux exchange of nutrients between ice and ocean by Jin et al. (2006a). The calculation of the flux is applied in each ice category as a function of bottom sea ice growth/melting rate, temperature, and salinity from CICE, and then a sum of the flux from all categories is used to communicate with the ocean ecosystem model. The tracer fluxes through the ice–ocean interface are calculated using flux velocity (T_{wi} by Jin et al., 2006a), which is a function of ice growth/melt rate. A small amount of ice algal seed concentration (0.2 mmol N m^{-3}) is assumed to be in the ocean and to be transported to the ice bottom layer and trapped there as initial algal biomass when the flux velocity is positive and ice algal biomass is less than 13 mmol N m^{-3}. (This number is chosen according to the observational data at the bottom of fast ice offshore Barrow before spring bloom by Jin et al. (2006a).) During ice melting, the ice algae are flushed into the ocean and treated as two parts: 10% becomes actively growing diatom, and the rest are not growing and are gradually decomposed to NH_4. This partition of ice algae is based on a concept from the field observation by Horner and Schrader (1982) that ice algal cells released from the ice into the water column were only marginally productive. A variation of the partition from 10% to 25% had only small impacts on annual pelagic primary production.

The pelagic ecosystem model is a medium-complexity NPZD-type model, which evolved from Moore et al. (2002, 2004) with multi-types of phytoplankton and nutrients to accommodate diverse ecological regimes around the globe. The advantages of this model are the following: (1) it is coupled with a state-of-the-art coupled ice–ocean physical model with continuing updates and large community support; (2) the global domain avoids the long open boundary settings around the Arctic Ocean; and (3) the ecosystem model has proved its ability to model biogeochemical cycles across diverse regimes.

3. Numerical setting for the 3-D coupled ice–ocean ecosystem model

The POP-CICE-ecosystem model runs on a global domain (displaced North Pole in Greenland (Hunke and Bitz, 2009)). There are 320 × 384 horizontal grid cells with grid space ranging between 20 and 85 km and averaging 40 km north of 70°N. There are 40 vertical layers in the ocean, and the layer thicknesses from the surface are 10.0, 10.1, 10.3, 10.6, 11.1, 11.7, 12.4, 13.3, 14.6, 16.2, 18.2, 20.8, 24.1, 28.6, 34.7, 43.2, 55.2, 72.3, 96.7, 130.0, 170.0, 208.0, 233.6, 245.3, 249.0, and the rest are 250.0.

Atmospheric forcing data include six-hourly air temperature, specific humidity, and wind velocity components from the Common Ocean Reference Experiments (CORE) version 2, 1958–2007 (Large and Yeager, 2009), along with monthly "normal year" precipitation from version 1 (Large and Yeager, 2004), as described by Hunke and Holland (2007). Shortwave radiation and light attenuation through snow and ice are calculated in each ice thickness category in the CICE before passing to the ecosystem modules.

Initial conditions for ocean variables (T and S) and biological variables (NO_3, Si) are from the gridded World Ocean Atlas (WOA2005, from the NOAA web site http://www.nodc.noaa.gov/OC5/WOD05/pr_wod05.html). Other ocean biological model initial conditions are the same as the global model simulation by Moore et al. (2004). Sea ice initial conditions for the physical model are from earlier runs (1958–2006) without the biological model (Hunke and Bitz, 2009). Initial conditions of nutrients at the bottom ice are set at the same as the sea surface water. The model is not sensitive to this setting because the total amount of nutrients that can be contained at the ice bottom is relatively small compared to the vast volume of the ocean.

The model runs from 1992 to 2007 and the first 6 yr are thought to be spin-up years. Because the interannual variations of the modeled ice area and extent have followed observations well since 1994, it is reasonable that the first 6 yr are enough for the sea ice model spin-up. The deep ocean might take longer to spin up, but it is adequate since the focus of this study is on the surface

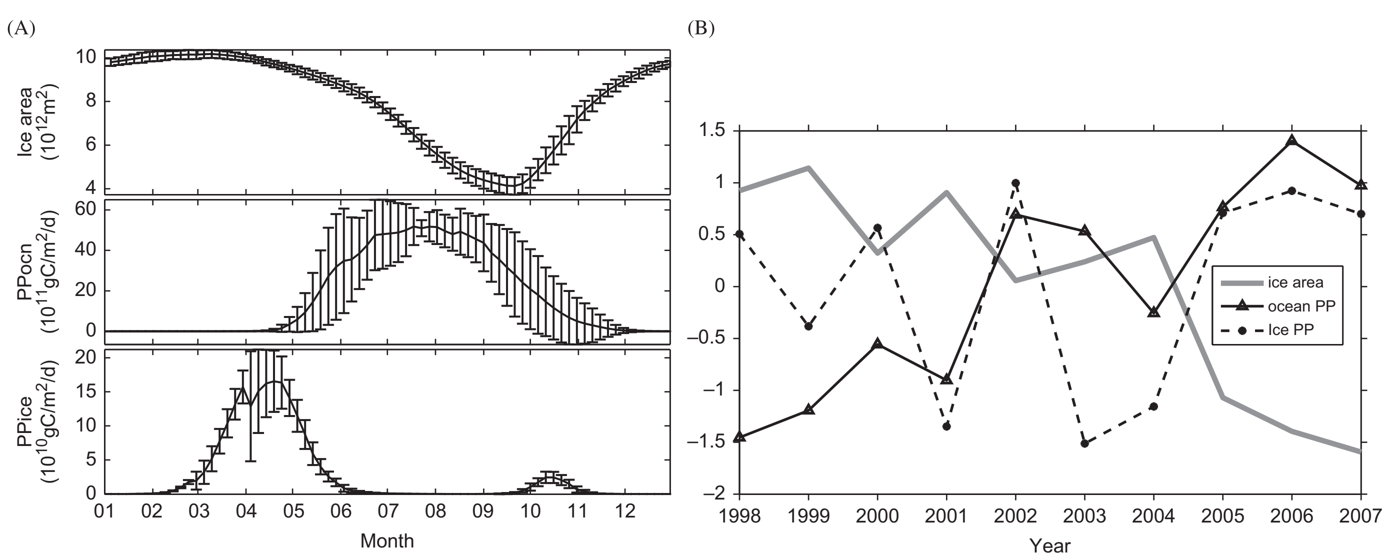

Fig. 3. Time series of modeled sea ice area, upper ocean 100 m integrated primary production and sea ice algal production within the Arctic Circle: (A) mean seasonal cycle of 1998–2007 and standard deviation and (B) normalized annual production. The normalization was done by minus the mean and divided by the standard deviation of the time series.

Please cite this article as: Jin, M., et al., Investigation of Arctic sea ice and ocean primary production for the period 1992–2007 using a 3-D global ice–ocean ecosystem model. Deep-Sea Research II (2011), doi:10.1016/j.dsr2.2011.06.003

100 m. The following discussions focus on the model results of the pan-Arctic region (Fig. 1A) from 1998 to 2007.

4. Results and discussion

4.1. Seasonal and interannual variations of the physical environment in the pan-Arctic

The seasonal and interannual changes of the total simulated and observed Northern Hemisphere sea ice cover from 1992 to 2007 are shown in Fig. 1B. The simulated ice area and ice extent match the seasonal minimum and maximum very well with satellite remote sensing data from the National Snow and Ice Data Center (NSIDC, http://nsidc.org/). The interannual changes of the total ice area are relatively small before 2002, but the ice area has decreased significantly since 2003.

4.2. Seasonal and interannual variations of sea ice and ocean primary production within the Arctic circle

The focus of this section is on the seasonal and interannual changes of marine primary production within the Arctic Circle (north of 66.56°N). The modeled monthly mean sea surface Chl-a in the open water showed reasonable timing and duration of the phytoplankton bloom close to the Sea-viewing Wide Field-of-view Sensor (SeaWiFS) data (http://oceancolor.gsfc.nasa.gov/SeaWiFS/) in most years (1998–2005), except for a later starting time of the modeled phytoplankton bloom in 2006 and 2007 (Fig. 2A). The model had a higher Chl-a bloom peak than SeaWiFS in some years. The differences of the Chl-a peak are within 10% in 1998, but 20–50% in the other years. Besides model errors, this difference may be partially caused by missing data during peak bloom time due to cloudy weather. The long-term mean Chl-a (1998–2007) was 0.75 mg/m^3 for the model and 0.8 mg/m^3 for the SeaWiFS, as shown by the two horizontal lines in Fig. 2A. These figures are within 10% deviation because they are less affected by the missing data.

The depth integrated primary production within the Arctic Circle has been derived using satellite remote sensing Chl-a data (since 1998) with an empirical algorithm (Arrigo et al., 2008a) developed specifically for the Arctic (Pabi et al., 2008). Using this method, Arrigo et al. (2008b) showed a 22% increase of open ocean primary production from about 410 to 510 T g C yr^{-1} from 2003 to 2007 due to the increased open water area in the Arctic. In comparison, our modeled results (Fig. 2B) showed a very close range of production and a 14% increase from 480 to 550 T g C yr^{-1} during the same period. The estimates for 1998–2006 averaged open-ocean upper 100 m primary production were 419 ± 33 Tg C yr^{-1} by remote sensing (Pabi et al., 2008) and 413 ± 88 Tg C yr^{-1} by this model simulation. The modeled annual mean production for 1998–2006 was very close to the estimates by remote sensing but with larger interannual variations.

The simulated sea ice area, ice algal production, and integrated upper 100 m ocean (including the ice-covered part of the ocean) production within the Arctic Circle from 1998 to 2007 were shown in mean seasonal cycles and standard deviations (Fig. 3A) and in time series of normalized annual mean (Fig. 3B). The durations of blooms were from March to early June for ice algae and May–September for phytoplankton (Fig. 3A). The distinct durations of ice and ocean production have important ecological effects on the arctic food web, as the

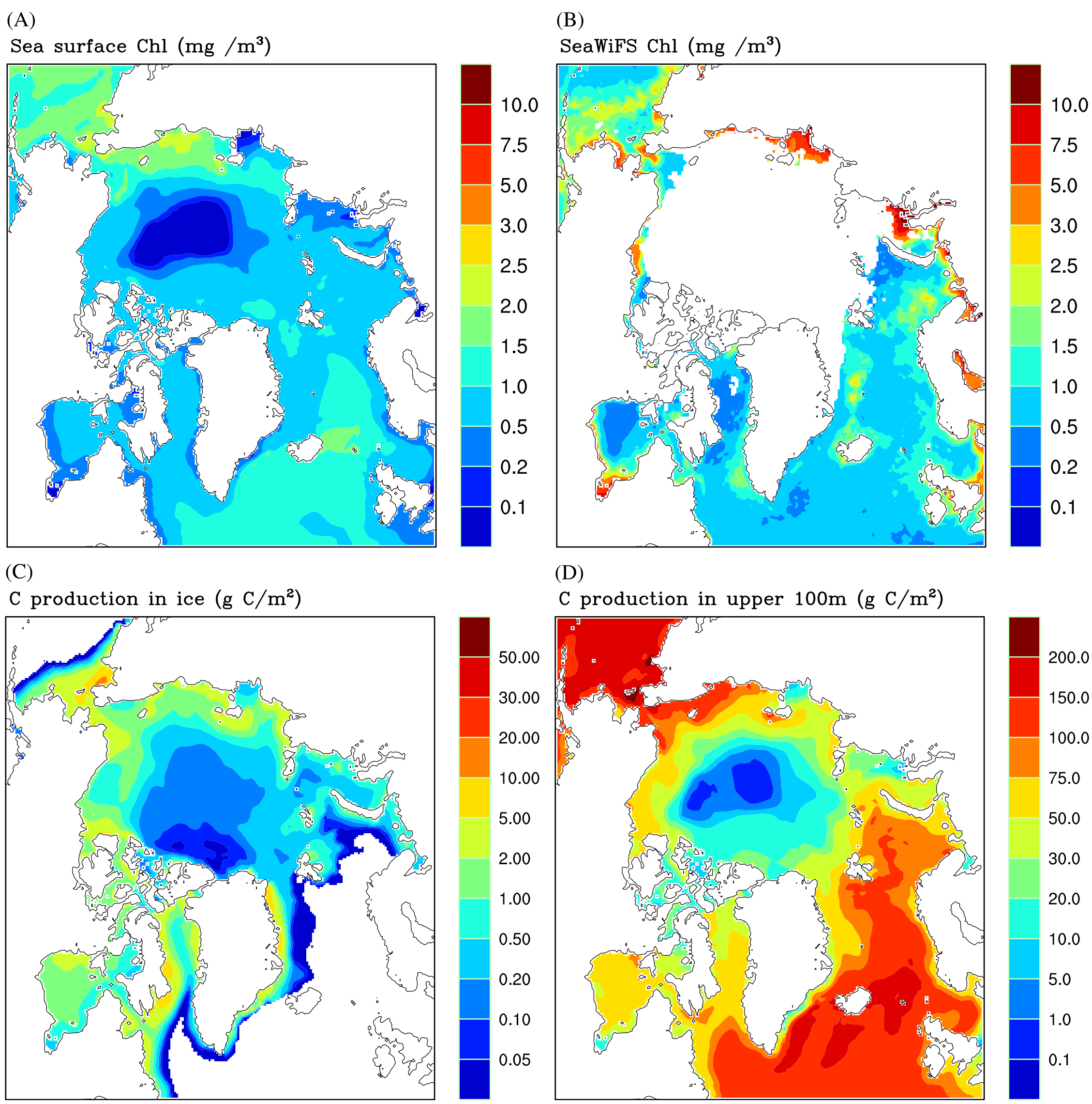

Fig. 4. Sea surface Chl-a averaged over 1998–2007 by (A) model and (B) SeaWiFS. Modeled pan-Arctic annual primary production averaged over 1998–2007 in (C) sea ice, (D) ocean upper 100 m.

Please cite this article as: Jin, M., et al., Investigation of Arctic sea ice and ocean primary production for the period 1992–2007 using a 3-D global ice–ocean ecosystem model. Deep-Sea Research II (2011), doi:10.1016/j.dsr2.2011.06.003

ice and ocean primary production complement each other in providing prolonged food support for the upper trophic level. The interannual variation was highest during the peak time of April for ice algae, but low in the peak time of July to mid-August for ocean production. The ocean production showed higher variations in June and September. Ice algal production started in early March when light became favorable and nutrient supply was plentiful. Ice melting from early June flushed ice algae out of ice and put an end to the ice algal bloom as melting became widespread in the Arctic. A small ice algal bloom in October was due to still available light in some regions and to growing ice habitat. The duration of ocean production from May to September agrees with the estimates by Pabi et al. (2008). The sharp decline of ocean production in September was the result of both declining light and increasing vertical mixing, which brought phytoplankton down to less favorable light conditions.

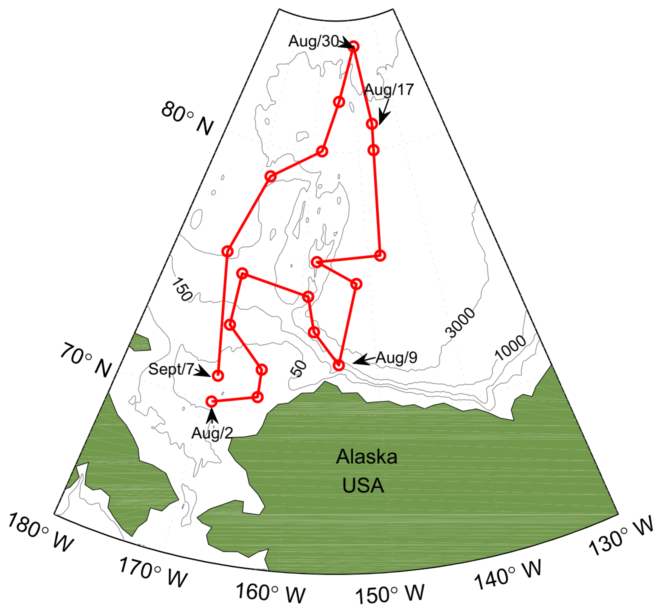

Fig. 5. Observational stations (the 19 dots) during August 2–September 7, 2008. The northern most station is 84°N reached on August 30. The dates of the 19 stations are August 2, 4, 4, 5, 6, 7, 8, 9, 11, 12, 14, 16, 17, 30, 31, September 1, 3, 5, and 7.

The annual mean ice algal production (Fig. 3B) showed a weak and insignificant negative correlation with ice area from 1998 to 2007 (correlation coefficient −0.56 and *p*-value 0.09), and there was even more ice algal production during low ice years from 2005 to 2007. The reason is that ice algal production is affected by the combined effects of ice growth/melt, nutrient availability, and light intensity, rather than simply being proportional to the ice area alone. There is a strong and significant negative correlation between overall ice area and ocean production (correlation coefficient −0.89 and *p*-value 0.0006). Ocean production in Fig. 3B includes water under sea ice (in differentiation to open water production mentioned in Fig. 2B), and its long-term trend has been opposite to the changes of ice area in most years. This indicates that overall Arctic Ocean primary production is likely to increase under the global warming trend as long as nutrients are not limited. The mean and standard deviations of the ocean and ice production were 627 ± 51 and 10.1 ± 2.0 Tg C yr^{-1} during 1998 to 2007. Ocean production under ice is only half of open-ocean production and has a smaller standard deviation.

4.3. Annual sea ice and ocean primary production in the pan-Arctic and model-data comparison

The modeled annual mean sea surface Chl-a averaged over 1998–2007 was compared to SeaWiFS data in Fig. 4A and B. There are two distinct regions of Chl-a concentration. One is the Bering Sea with high productivity (1–3 mg/m^3), where the model showed similar mean Chl-a but a lower maximum along the Shelf Break and higher on the shelf regions. The other is the North Atlantic Ocean with Chl-a between 0.5 and 1.5 mg/m^3 in most regions for both the model and the SeaWiFS data. The model showed higher value in Baffin Bay and Hudson Bay, but lower value in the Barents Sea. The high values of SeaWiFS data in some coastal regions (e.g., the mouths of the Yukon, Lena, Yenisey, and Mackenzie rivers) might be biased high due to the influence of riverine sediments and/or colored dissolved organic matter that have the potential to alter optical properties in coastal waters (Pabi et al., 2008; Zhang et al., 2010).

The simulated pan-Arctic annual mean primary production (average of 1998–2007) in sea ice and the upper 100 m of ocean are shown in Fig. 4C and D. The modeled annual ice algal production (Fig. 4C) was around 2 g C m^{-2} yr^{-1}, within the observed ranges of 0.7–5 g C m^{-2} yr^{-1} offshore Barrow in the Chukchi Sea (Jin et al., 2006a). The modeled production in the Canadian Basin was much lower than the Chukchi as observed by Lee et al. (2010). This is due to multiple factors, such as lower light intensity reaching the ice surface, thicker ice and lower light at the ice bottom, and lower nitrate concentration in the surface ocean than in the surrounding shelf regions. The modeled annual ice algal production for the entire pan-Arctic ranged from 15.2 to 24.3 T g C yr^{-1} from 1998 to 2007. The mean was 21.3 T g C yr^{-1}, which is in the range of multi-observational estimations of 9–73 T g C yr^{-1} (Legendre et al., 1992) and twice the ice algal production within the Arctic Circle.

The integrated ocean production (Fig. 4D) revealed high production in large areas of the Bering Sea (> 150 g C m^{-2} yr^{-1}), and some of the highest production

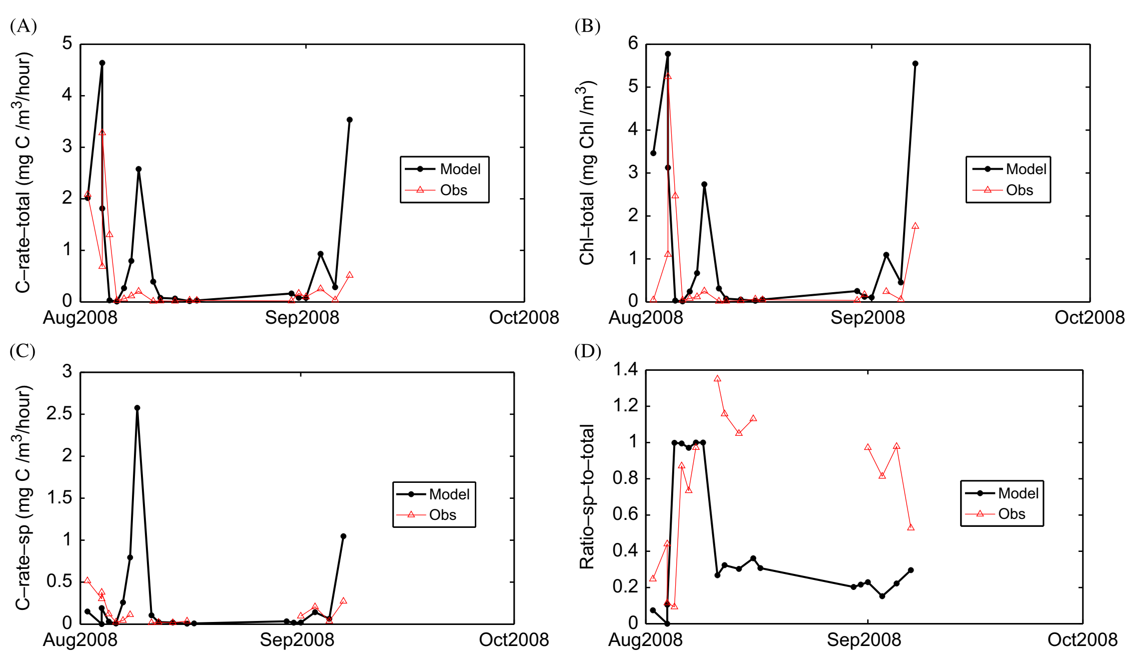

Fig. 6. Model-data comparison of (A) total carbon uptake rate, (B) total Chl-a, (C) small phytoplankton carbon uptake rate, and (D) ratio of small to total phytoplankton carbon uptake rate. All variables are averaged in the sea surface 10 m. There are 19 data points in each line (note Fig. 6B–D contain missing data points) correspoinding to the cruise stations in Fig. 5.

Please cite this article as: Jin, M., et al., Investigation of Arctic sea ice and ocean primary production for the period 1992–2007 using a 3-D global ice–ocean ecosystem model. Deep-Sea Research II (2011), doi:10.1016/j.dsr2.2011.06.003

(>200 g C m^{-2} yr^{-1}) in the Anadyr Water on the western side of the northern Bering Sea due to high nitrate concentration (Sambrotto et al., 1984; Lee et al., 2007). The modeled ocean production in the Chukchi ranged from 150 g C m^{-2} yr^{-1} near Bering Strait down to about 50 g C m^{-2} yr^{-1} at the shelf break, within the range 55–145 g C m^{-2} yr^{-1} observed in the Chukchi Sea in 2002–2004 (Springer and McRoy, 1993; Lee et al., 2007). The modeled production was 30–100 g C m^{-2} yr^{-1} in the Beaufort Sea shelf and Siberian shelf, and mostly below 20 with a minimum less than 1 g C m^{-2} yr^{-1} in the perennially ice-covered central Arctic. These spatial variations of production were within the observed ranges reported by Wheeler et al. (1996) and Gosselin et al. (1997). The total annual primary production (phytoplankton plus ice algae) in the central Arctic Ocean is about 15 g C m^{-2} yr^{-1}, which is at least one order of magnitude greater than estimates (phytoplankton only) by Apollonio (1959); English (1961). The measurements in the 1950s may have underestimated the production due to the changes of the procedural details of the ^{14}C method after the 1950s (Pomeroy, 1997). The model showed large spatial variations spanning the measurement ranges in the 1950s to the 1990s.

The primary production rates for small phytoplankton and total phytoplankton and total Chl-a were observed during an arctic cruise on the ship *XueLong* from August 12 to September 7, 2008 (cruise track shown in Fig. 5). Since the model forcing data were available only to 2007, the model results (surface 10m layer) in 2007 were used to compare with the observational data averaged over the upper 10 m. The model captured the observed high carbon production rate (maximum of 3.3 mg C m^{-3} h^{-1}) and high spatial variations in the Chukchi Sea and the low rate (lower than 0.2 mg C m^{-3} h^{-1}) in most of the Canadian Basin (Fig. 6). The time series of the total Chl-a concentration (Fig. 6B) was generally proportional to that of the total primary production rate. The high Chl-a concentration was about 5.3 mg Chl m^{-3} in the Chukchi Shelf for both model and observation. The Chl-a was lower than 0.3 mg Chl m^{-3} at all observational stations and most of the modeled points in the Canadian Basin, except for one high value over 2 mg Chl m^{-3}. This may be caused by its close location to the Beaufort Sea coast (near Barrow) between high and low productivity areas, and a high value was picked from the model results. The last point is in the Chukchi Sea (Fig. 5), and the modeled Chl-a was much higher than those in the central Arctic. Observed Chl-a at the last point showed a similar increase but with less magnitude than the modeled.

The small phytoplankton carbon uptake rate was higher in the Chukchi Sea than in the Canadian Basin (Fig. 6C), similar to that of the total phytoplankton carbon uptake rate. The observed ratios of small to the mean of all phytoplankton carbon uptake rates were less than 0.4 in the Chukchi Sea shelf but around 1 in the Canadian Basin (Fig. 6D), but the model captured this transition of species composition only in the first 7 stations. More study is needed to determine if the spatial distribution of phytoplankton species composition holds true in other months and years.

4.4. Changes of sea ice and ocean primary production between high and low ice years

The arctic sea ice decreased significantly from 1998 to 2007, and ice and ocean primary production increased in the same time, as shown in Fig. 3B. To find the spatial distribution of the production differences between the high and low ice years, five low ice years (2002, 2003, and 2005–2007) out of the 10 yr of model results (1998–2007) were chosen according to their lower mean ice area from May to

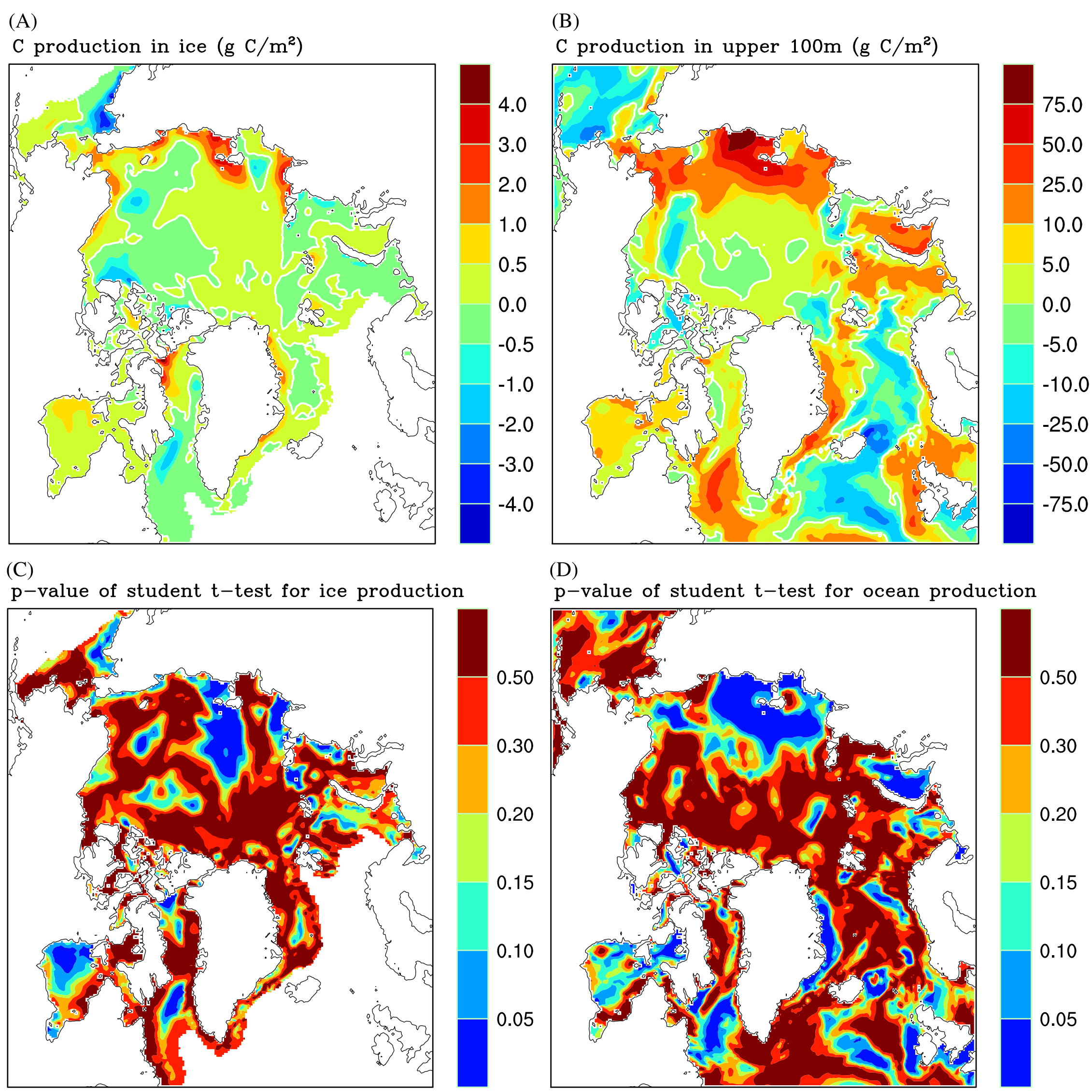

Fig. 7. Modeled pan-Arctic annual primary production difference by the mean of the low ice years (2002, 2003, and 2005–2007) minus the mean of the high ice years (1998–2001 and 2004) in (A) sea ice, (B) ocean upper 100 m. The white contour lines denote zero-value. (C) and (D) are the *p*-value of student *t*-test of the difference in (A) and (B).

Please cite this article as: Jin, M., et al., Investigation of Arctic sea ice and ocean primary production for the period 1992–2007 using a 3-D global ice–ocean ecosystem model. Deep-Sea Research II (2011), doi:10.1016/j.dsr2.2011.06.003

September according to the model results and the NSIDC ice area data. Those 5 yr also have lower September minimum ice area than the remaining five high ice years (1998–2001 and 2004). The difference in modeled annual primary production was calculated by the low ice year mean minus the high ice year mean, and the *p*-value of the student *t*-test was calculated to show the significance of the difference (Fig. 7). A similar difference in the mean September minimum sea ice concentration of the warm and cold years is shown in Fig. 8. Most of the of sea ice loss was in the shelf seas on the Russian side (Chukchi Sea to East Siberian Sea, Laptev Sea, and Kara Sea), and the Arctic Basin showed mixed areas of increase and decrease.

Ice algal production in low ice years was much higher on the Alaskan and Siberian coasts and Hudson Bay and only slightly higher in the central Arctic (Fig. 7A) due to increased light availability through thinner ice in low ice years. The statistical *t*-test (Fig. 7C) showed only the increase of production in the areas of the Siberian coast to the central Arctic and Hudson Bay with over 95% (1–*p*-value) confidence. Ice production was lower in the west side of the Bering Sea and south of Baffin Bay with over 95% confidence.

The ocean production difference (Fig. 7B) in the low ice years showed an increase in most of the Arctic shelf seas including Hudson Bay, and a decrease in the Bering Sea, Beaufort Sea, and most of the open water areas of the North Atlantic Ocean. The increase in ocean production on the Arctic shelf was due to increased open water area and growing season, similar to the ocean production increase due to decreasing sea ice from 2003 to 2007 (Arrigo et al., 2008b). The East Siberian and Laptev seas showed the most significant ocean production increase (Fig. 7B and D) corresponding to sea ice loss (Fig. 8). The production decrease at lower latitude and increase at higher latitude indicated a northward movement of the ocean production in low years. The decrease at lower latitude may be caused by decreased vertical mixing and thus fewer nutrients in the euphotic zone for production due to ocean warming. During 2005–2007, the northward movement of production was evident from the south (Bering Sea and open areas of the North Atlantic Ocean) to the Arctic shelf seas but not in the Beaufort Sea and the central Arctic Basin. The statistical *t*-test (Fig. 7D) showed a confidence level over 95% in areas of the Chukchi Sea and Siberian Sea and two small areas in the Bering Sea, where some observational evidence indicates a trend of ecological changes. However, historical observations, which span a longer time period than the model, showed that ocean production in the Bering Sea decreased from 250–470 $g\,C\,m^{-2}\,yr^{-1}$ a decade ago (Hansell and Goering, 1990; Hansell et al., 1993; Springer and McRoy, 1993; Springer et al., 1996) to 144 $g\,C\,m^{-2}\,yr^{-1}$ in recent years (Lee et al., 2007). Decreasing production in the Bering Sea in the last decades was accompanied by increases in the Chukchi and Siberian seas. Signs of the ecological effects of this decadal northward shift of production were also seen in the northward migration of marine mammal populations in the northern Bering Sea (Grebmeier et al., 2006).

The spatially low confidence levels of production differences between high and low ice years in most areas may be due to the fact that the spatial distribution of sea ice area varied from year to year and also seasonally during the major bloom period from March to September. The correlation is low in thick ice areas (e.g., Canadian Archipelago and the adjacent Arctic Ocean) and permanently open waters (e.g., North Atlantic). This indicates that the impacts of declining sea ice area at current levels are still limited to thin ice and the marginal ice zone. Still it is possible that, as global warming deepens, these impacts may reach thick ice areas as well. Even though the spatial distribution of differences in production is uneven, the overall integrated ice and ocean production within the Arctic Circle has been increasing with declining sea ice area. The trend of ocean production is stronger and more significant than that of ice production, as discussed in Fig. 3B.

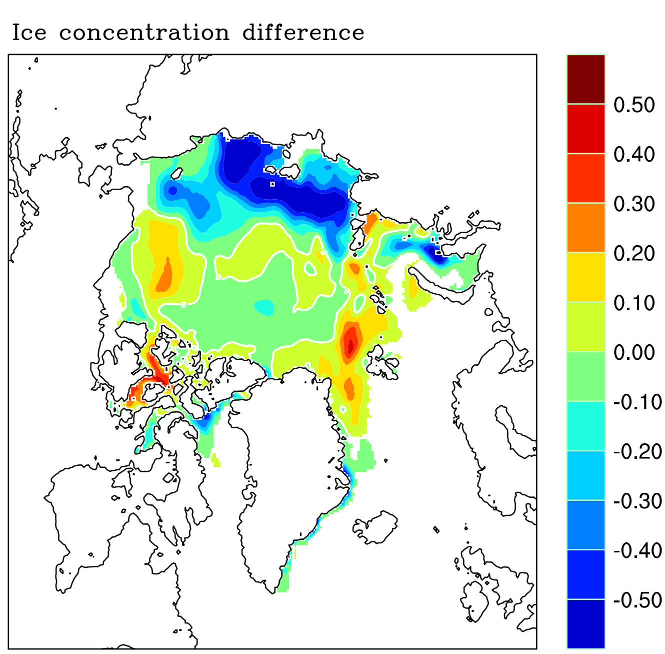

Fig. 8. Modeled September ice area difference by the mean of the low ice years (2002, 2003 and 2005–2007) minus the mean of the high ice years (1998–2001 and 2004).

5. Conclusions

In the Arctic Ocean, sea ice algal production, although smaller than ocean algal production, is an ecologically important source of food to the upper trophic level during the long winter before ice melt. In this study, an ice algal ecosystem model was added to fully couple with the global physical model POP-CICE and the open-ocean pelagic ecosystem model. Forced by atmospheric data from National Centers for Environmental Prediction (NCEP), the physical model well captured the seasonal and interannual variations of northern hemispheric sea ice extent and areas detected by satellite remote sensing during the model period of 1992–2007.

The model results revealed a mean seasonal cycle of ice algal production from March to May and subsequent ocean production from May to September in the Arctic during 1998–2007. The simulated mean open-ocean upper 100 m primary production within the Arctic Circle was $413 \pm 88\,T\,g\,C\,yr^{-1}$ in 1998–2006. This was close to the remote sensing derived estimate of $419 \pm 33\,Tg\,C\,yr^{-1}$ but with higher interannual variations. The mean sea ice algal production in the Northern Hemisphere was 21.3 $T\,g\,C\,yr^{-1}$ from 1992 to 2007, which is in the range of multi-observational estimates of 9–73 $Tg\,C\,yr^{-1}$ by in situ measurements.

In the western Arctic, both sea ice and ocean primary production show a northward slope from the highest in the Bering Sea to the lowest in the central Arctic. The modeled productivity of small phytoplankton was lower than that of large phytoplankton in the Chukchi Sea shelf, but it was higher in the Beaufort Sea in August. More study is needed to confirm findings in different regions and at different times.

Significant changes in the arctic ecosystem due to rising temperature and increasing open water areas have been observed with various observational tools in recent decades. Model results reveal an increase of open-ocean primary production from 2003 to 2007 in the Arctic. They also show a northward shift of ocean primary production from the Bering Sea to the Arctic shelf if the sea ice area decreases. This trend was seen in various in situ observations in the last two decades in the Bering Sea shelf. Marine mammal populations also showed a trend of northward migration in the northern Bering Sea (Grebmeier et al., 2006).

The model has some limitations that need to be improved in the future study. The physical model of this study is based on the coarse horizontal resolution climate models (POP-CICE as components of the NCAR climate model). The ecosystem model results may be improved by increasing horizontal and vertical resolutions, as the model can resolve better important narrow straits and topography. Inclusion of tidal mixing in the model is also important for simulating nutrient transportation and primary production in shallow shelf regions like the Bering Sea shelf (Jin et al., 2006b). Some compartments in the model, such as oxygen O2, alkalinity ALK, DMS, DMSP, etc., are calculated but not discussed in this study. They are important for understanding ecosystem functioning and the linkage between ecosystem and climate changes, and they will be discussed in further studies.

Acknowledgments

This work was supported under the IARC-JAMSTEC Agreement, the DOE EPSCoR program DE-FG02-08ER46502, NSF ARC-0652838, and KOPRI-PM09020. The Chinese ship *Xuelong* and crew's support are appreciated.

References

Apollonio, S., 1959. Hydrobiological measurements on IGY Drifting Station Bravo. Trans. Am. Geophys. Union 40, 316–319.

Arrigo, K.R., Kremer, J.N., Sullivan, C.W., 1993. A simulated Antarctic fast ice ecosystem. J. Geophys. Res. 98 (C4), 6929–6946.

Arrigo, K.R., Sullivan, C.W., 1994. A high-resolution bio-optical model of microalgal growth: tests using sea-ice algal community time-series data. Limnol. Oceanogr. 39 (3), 609–631.

Arrigo, K.R., Worthen, D.L., Lizotte, M.P., Dixon, P., Dieckmann, G., 1997. Primary production in Antarctic sea ice. Science 276 (5311), 394–397.

Arrigo, K.R., van Dijken, G.L., Bushinsky, S., 2008a. Primary production in the Southern Ocean, 1997–2006. J. Geophys. Res. 113, C08004. doi:10.1029/2007JC004551.

Arrigo, K.R., van Dijken, G., Pabi, S., 2008b. Impact of a shrinking Arctic ice cover on marine primary production. Geophys. Res. Lett. 35, L19603. doi:10.1029/2008GL035028.

Bluhm, B., Gradinger, R., 2008. Regional variability in food availability for Arctic marine mammals. Ecol. Appl. 18, S77–S96.

Deal, C., Jin, M., Elliott, S., Hunke, E., Maltrud, M., Jeffery, N., Large-scale modeling of primary production and ice algal biomass within Arctic sea ice in 1992. J. Geophys. Res., in press, doi:10.1029/2010JC006409.

English, T.S., 1961. Some biological oceanographic observations in the central North Polar Sea Drift Station Alpha, 1957–9158. Arct. Inst. North Am. Res. Pap. 13, 1–80.

Gosselin, M., Levasseur, M., Wheeler, P.A., Horner, R.A., Booth, B.C., 1997. New measurements of phytoplankton and ice algal production in the Arctic Ocean. Deep-Sea Res. II 44, 1623–1644.

Grebmeier, J.M., Overland, J.E., Moore, S.E., Farley, E.V., Carmack, E.C., Cooper, L.W., Frey, K.E., Hell, J.H., McLaughlin, F.A., McNutt, S.L., 2006. A major ecosystem shift in the northern Bering Sea. Science 311, 1461–1464.

Hansell, D.A., Goering, J.J., 1990. Pelagic nitrogen flux in the northern Bering Sea. Cont. Shelf Res. 10, 501–519.

Hansell, D.A., Whitledge, T.E., Goering, J.J., 1993. Patterns of nitrate utilization and new production over the Bering-Chukchi shelf. Cont. Shelf Res. 13, 601–627.

Horner, R., Schrader, G.C., 1982. Relative contributions of ice algae, phytoplankton, and benthic microalgae to primary production in nearshore regions of the Bearfort Sea. Arctic 35, 485–503.

Hunke, E.C., Holland, M.M., 2007. Global atmospheric forcing data for Arctic ice–ocean modeling. J. Geophys. Res. 112, C04S14. doi:10.1029/2006JC003640.

Hunke, E.C., Lipscomb, W.H., 2008. CICE: The Los Alamos Sea Ice Model: Documentation and Software User's Manual, version 4.0, Technical Report LA-CC-06-012, Los Alamos National Laboratory, Los Alamos, NM.

Hunke, E.C., Bitz, C.M., 2009. Age characteristics in a multidecadal Arctic sea ice simulation. J. Geophys. Res. 114, C08013. doi:10.1029/2008JC005186.

Jin, M., Deal, C.J., Wang, J., Shin, K.H., Tanaka, N., Whitledge, T.E., Lee, S.H., Gradinger, R.R., 2006a. Controls of the landfast ice–ocean ecosystem offshore Barrow, Alaska. Ann. Glaciol. 44, 63–72.

Jin, M., Deal, C.J., Wang, J., Tanaka, N., Ikeda, M., 2006b. Vertical mixing effects on the phytoplankton bloom in the southeastern Bering Sea mid-shelf. J. Geophys. Res. 111, C03002. doi:10.1029/2005JC002994.

Jin, M., Deal, C., Wang, J., Alexander, V., Gradinger, R., Saitoh, S., Iida, T., Wan, Z., Stabeno, P., 2007. Ice-associated phytoplankton blooms in the southeastern Bering Sea. Geophys. Res. Lett. 34, L06612. doi:10.1029/2006GL028849.

Jin, M., Deal, C.J., Wang, J., McRoy, C.P., 2009. Response of lower trophic level production to long-term climate change in the southeastern Bering Sea. J. Geophys. Res. 114, C04010. doi:10.1029/2008JC005105.

Large, W., Yeager, S., 2004. Diurnal to decadal global forcing for ocean and sea-ice models: the data sets and flux climatologies. Technical Note NCAR/TN-460+STR, Climate and Global Dynamics Division, National Center For Atmospheric Research, Boulder, Colorado.

Large, W., Yeager, S.G., 2009. The global climatology of an interannually varying air–sea flux data set. Clim. Dyn. 33, 341–364.

Lavoie, D., Denman, K., Michel, C., 2005. Modeling ice algal growth and decline in a seasonally ice-covered region of the Arctic (Resolute Passage, Canadian Archipelago). J. Geophys. Res. 110, C11009 doi:10.1029.2005JC002922.

Lee, H.S., Whitledge, T.E., Kang, S., 2007. Recent carbon and nitrogen uptake rates of phytoplankton in Bering Strait and the Chukchi Sea. Cont. Shelf Res. 27, 2231–2249.

Lee, H.S., Jin, M., Whitledge, T.E., 2010. Comparison of bottom sea-ice algal characteristics from coastal and offshore regions in the Arctic Ocean. Pol. Biol.. doi:10.1007/s00300-010-0820-1.

Legendre, L., Ackley, S.F., Dieckmann, G.S., Gullicksen, B., Horner, R., Hoshiai, T., Melnikov, I.A., Reeburgh, W.S., Spindler, M., Sullivan, C.W., 1992. Ecology of sea ice biota—Part 2: global significance. Pol. Biol. 12, 429–444.

Li, W.K.W., McLaughlin, F.A., Lovejoy, C., Carmack, E.C., 2009. Smallest algae thrive as the Arctic Ocean freshens. Science 326 539–539.

Moore, J.K., Doney, S.C., Kleypas, J.C., Glover, D.M., Fung, I.Y., 2002. An intermediate complexity marine ecosystem model for the global domain. Deep-Sea Res. II 49, 403–462.

Moore, J.K., Doney, S.C., Lindsay, K., 2004. Upper ocean ecosystem dynamics and iron cycling in a global three-dimensional model. Global Biogeochem. Cycles 18, GB4028. doi:10.1029/2004GB002220.

Pabi, S., van Dijken, G.L., Arrigo, K.R., 2008. Primary production in the Arctic Ocean, 1998–2006. J. Geophys. Res. 113, C08005. doi:10.1029/2007JC004578.

Pomeroy, L.R., 1997. Primary production in the Arctic Ocean estimated from dissolved oxygen. J. Mar. Syst. 10, 1–8.

Sambrotto, R.N., Goering, J.J., McRoy, C.P., 1984. Large yearly production of phytoplankton in the western Bering Strait. Science 225, 1147–1150.

Springer, A.M., McRoy, C.P., 1993. The paradox of pelagic food webs in the northern Bering Sea—III. Patterns of primary production. Cont. Shelf Res. 13, 575–599.

Springer, A.M., McRoy, C.P., Flint, M.V., 1996. The Bering Sea Green Belt: shelf-edge processes and ecosystem production. Fish. Oceanogr. 5, 205–223.

Vezina, A.F., Demers, S., Laurion, I., Sime-Ngando, T., Juniper, S.K., Devine, L., 1997. Carbon flows through the microbial food web of first-year ice in Resolute Passage (Canadian High Arctic). J. Mar. Syst. 11 (1–2), 173–189.

Walsh, J.J., Dieterlea, D.A., Maslowskib, W., Grebmeierc, J.M., Whitledged, T.E., Flinte, M., Sukhanovae, I.N., Batesf, N., Cotag, G.F., Stockwelld, D., Moranh, S.B., Hanselli, D.A., McRoy, C.P., 2005. A numerical model of seasonal primary production within the Chukchi/Beaufort seas. Deep-Sea Res. II 52 (24–26), 3541–3576. doi:10.1016/j.dsr2.2005.09.009.

Walsh, J.E., 2008. Climate of the Arctic environment. Ecol. Appl. 18, S3–S22.

Wheeler, P.A., Gosselin, M., Sherr, E., Thibault, D., Kirchman, D.L., Benner, R., Whitledge, T., 1996. Active cycling of organic carbon in the central Arctic Ocean. Nature 380, 697–699.

Zhang, J., Spitz, Y.H., Steele, M., Ashjian, C., Campbell, R., Berline, L., Matrai, P., 2010. Modeling the impact of declining sea ice on the Arctic marine planktonic ecosystem. J. Geophys. Res. 115, C10015. doi:10.1029/2009JC005387.